

## Least-weight design of tow-steered composites

Dario Zamani<sup>1,a\*</sup>

<sup>1</sup>Politecnico di Torino, Corso Duca degli Abruzzi, 10129, Turin, Italy

<sup>a</sup>dario.zamani@polito.it

**Keywords:** Variable Stiffness Composites, Unified Formulation, Discrete Optimization, Least-Weight

**Abstract.** Automatic Fiber Placement (AFP) enables spatial variation of fiber orientation, enhancing mechanical performance compared to traditional composites. Variable Angle Tow (VAT) or Variable Stiffness Composites (VSC) optimize structural efficiency, which is crucial for lightweight aerospace structures. However, it is important to consider that limitations resulting from the manufacturing process can significantly impact the design domain available. This study proposes a mixed-integer optimization approach integrating the Carrera Unified Formulation (CUF) to minimize laminate weight while meeting frequency performance. This research aims to determine the optimal number of layers and lamination angles, considering manufacturing constraints and evaluating the impact of the selection of structural theory on the solutions.

### Introduction

In contrast to conventional straight fiber laminates, Variable Stiffness Composites (VSCs) provide designers with a notably expanded design space by enabling control over the fiber tows along conforming curvilinear paths. However, due to the inherently non-uniform stiffness properties of the computational domain, resulting in increased computational costs, it is imperative to develop suitable and efficient optimization and design tools. Groh and Weaver [1] addressed the issue of reducing the mass of VAT laminates produced by Continuous Tow Shearing (CTS). In particular, a genetic algorithm (GA) was combined with pattern searching, creating a hybrid optimization approach that reduced weight by 31% compared to traditional straight-fiber composites. Catapano et al. [2] proposed a two-level optimization strategy for VAT laminates that considers manufacturing requirements for Fused Filament Fabrication (FFF) and Continuous Filament Fabrication (CFF) techniques. The strategy involved multi-scale optimization and emphasized incorporating technological constraints into the design optimization process. In addition, Sánchez-Majano and Pagani [3] implemented the Carrera Unified Formulation (CUF) to construct a surrogate that mimicked the objective function to maximize the buckling load and the fundamental frequency of the VAT plates. This method provided the advantage of obtaining a model whose accuracy was determined by the appropriate choice of the order of the structural theory adopted. Lastly, Pagani et al. [4] developed a surrogate optimization framework to maximize the first natural frequency of VAT laminates, taking into account the presence of gaps and overlaps by combining the CUF with the Defect Layer Method (DLM) [5] directly into the optimization process.

This work aims to present a mixed-integer optimization strategy specifically designed to select the least-weight design of a VAT laminate while also maximizing the first natural frequency. The research has two main objectives: to determine how the manufacturing constraints affect the minimum number of layers needed to meet fundamental frequency requirements and to examine how the selection of structural theory affects optimal solutions.



### Unified finite elements for VSCs

In this work, CUF formalism is used to implement 2D FE. Specifically, as stated in [6], the 3D displacement field can be expressed using arbitrary through-the-thickness expansion functions  $F_\tau(\mathbf{z})$  as follows:

$$\mathbf{u}(x, y, z) = F_\tau(z)\mathbf{u}_\tau(x, y). \tau = 1, \dots, M \quad (1)$$

The symbol  $M$  represents the number of expansion terms, and  $\mathbf{u}_\tau(x, y)$  represents the vector containing the generalized displacements, with  $\tau$  indicating summation. Examining multi-layered structures typically employs either an Equivalent-Single-Layer (ESL) or Layer-Wise (LW) approach. In this manuscript, ESL models utilize Taylor polynomials represented by  $F_\tau(z)$ ; while LW employs Lagrange polynomials over individual layers and ensures the continuity of displacements at layer interfaces. Utilizing the FE and shape functions  $N_i(x, y)$ , the displacement field becomes:

$$\mathbf{u}(x, y, z) = N_i(x, y)F_\tau(z)\mathbf{q}_{\tau i}(x, y). i = 1, \dots, N_n \quad (2)$$

In Eq. (2),  $\mathbf{q}_{\tau i}$  are the unknown nodal variables, with  $N_n$  denoting the number of nodes per element. This work employs 2D nine-node quadratic elements for the in plane discretization.

The governing equations are derived using the Principle of Virtual Displacements (PVD), which asserts that the virtual variation of internal strain energy,  $\delta\mathcal{L}_{int}$ , equals the virtual work of external forces,  $\delta\mathcal{L}_{ext}$ , minus inertia forces,  $\delta\mathcal{L}_{ine}$ . Specifically,  $\delta\mathcal{L}_{int}$  can be written as:

$$\delta\mathcal{L}_{int} = \delta\mathbf{q}_{sj}^T \left[ \int_V \mathbf{D}^T(N_j F_s) \tilde{\mathbf{C}} \mathbf{D}(N_i F_\tau) dV \right] \mathbf{q}_{\tau i} = \delta\mathbf{q}_{sj}^T \mathbf{k}_0^{ij\tau s} \mathbf{q}_{\tau i}, \quad (3)$$

where  $\mathbf{k}_0^{ij\tau s}$  is the  $3 \times 3$  Fundamental Nucleus (FN) of the stiffness matrix, invariant regardless of 2D shape function order and through-the-thickness expansion.  $\mathbf{D}(\cdot)$  is the differential operator matrix with geometric relations, and  $\tilde{\mathbf{C}}$  is the material stiffness matrix in the global reference frame, i.e.,  $\tilde{\mathbf{C}} = \mathbf{T}(x, y)^T \mathbf{C} \mathbf{T}(x, y)$ . As fibers vary point-wise within the plane, the rotation matrix  $\mathbf{T}$  also varies accordingly. The virtual work of the inertia forces can be expressed as:

$$\delta\mathcal{L}_{ine} = \delta\mathbf{q}_{sj}^T \left[ \int_V \rho \mathbf{I} N_i N_j F_\tau F_s dV \right] \dot{\mathbf{q}}_{\tau i} = \delta\mathbf{q}_{sj}^T \mathbf{m}^{ij\tau s} \dot{\mathbf{q}}_{\tau i}, \quad (4)$$

in which  $\mathbf{I}$  denotes the  $3 \times 3$  identity matrix and  $\mathbf{m}^{ij\tau s}$  is the  $3 \times 3$  FN of the mass matrix. Thus, the undamped free vibration problem is expressed as follows:

$$\mathbf{M}\ddot{\mathbf{q}} + \mathbf{K}\mathbf{q} = 0. \quad (5)$$

In Eq. (8),  $\mathbf{M}$  and  $\mathbf{K}$  are the overall mass and stiffness matrices, respectively, obtained by iterating over FN's with indices  $i, j, \tau$  and  $s$  to compute element-level matrices, which are then assembled for the global structure. By applying harmonic solutions  $\mathbf{q} = \tilde{\mathbf{q}}e^{i\omega t}$ , Eq. (8) becomes:

$$(\mathbf{K} - \omega_i^2 \mathbf{M})\tilde{\mathbf{q}}_i = 0 \quad (6)$$

where  $\omega_i$  and  $\tilde{\mathbf{q}}_i$  are the  $i^{th}$  natural frequency and eigenvector, respectively.

### Optimization framework

This manuscript considers the multi-objective optimization of VSCs, which aims to minimize the weight and, therefore, the number of layers in the laminate while maximizing the first natural frequency. The plies that make up the laminate are varied for each evaluation of the objective function, along with the lamination angles  $T_0$  and  $T_1$  for each layer considered. Following the linearly varying fiber formulation [7],  $T_0$  represents the fiber angle at the plate's center, while  $T_1$  represents the angle at the edge. Both the unconstrained and the constrained problem are

considered. The maximum curvature of the AFP machine is chosen as the constraint of the optimization problem. Therefore, the local fiber curvature  $\kappa$  must be less than  $\kappa_{lim} = 3.28 \text{ m}^{-1}$ , as seen in Eq. (7).

$$\kappa = \frac{2(T_1 - T_0)}{a} \cos \left( (T_1 - T_0) \frac{x}{a/2} + T_0 \right) \leq 3.28 \text{ m}^{-1} \quad (7)$$

The NSGA-II algorithm is utilized to solve the optimization problem. The variables  $T_0$  and  $T_1$  can continuously vary between  $-90^\circ$  and  $90^\circ$ , while the number of plies  $N_{ply}$  can discretely vary between 6 and 10 layers. At each iteration, input files for structural analysis are created, and the natural frequency is then evaluated using the CUF-based FE code, as described in Section 2. The process is repeated iteratively until convergence.

### Results

This work aims to minimize the mass of a traditional 8-layer symmetrical straight fiber composite with optimum lamination  $\theta = [0^\circ, 90^\circ, 0^\circ, 90^\circ]_S$ , found in [8], while also fulfilling first natural frequency performance. The width and length of the plate are  $a = b = 0.5 \text{ m}$ , and each ply has a thickness of  $0.159 \text{ mm}$ . A fully clamped boundary condition was imposed on all four sides. The reference mass is  $m_{ref} = 0.5247 \text{ kg}$ , while the optimum frequency is  $f_{ref} = 54.68 \text{ Hz}$ . The convergence analysis performed in [4] suggests that a  $6 \times 6$  Q9 FE mesh effectively captures the fundamental frequency, requiring relatively low computational effort, which facilitates the reduction of the computational burden associated with the optimization process.

Table 1. Optimal design results for the unconstrained problem

	ESL – TE 1	ESL – TE 3	LW – LD2
$\langle T_0, T_1 \rangle^1 [^\circ]$	$\langle -90, 6 \rangle$	$\langle -90, 7 \rangle$	$\langle -90, 6 \rangle$
$\langle T_0, T_1 \rangle^2 [^\circ]$	$\langle 90, -9 \rangle$	$\langle 90, -9 \rangle$	$\langle 90, -9 \rangle$
$\langle T_0, T_1 \rangle^3 [^\circ]$	$\langle 90, -9 \rangle$	$\langle 90, -8 \rangle$	$\langle 90, -9 \rangle$
$\langle T_0, T_1 \rangle^4 [^\circ]$	$\langle -90, 6 \rangle$	$\langle -90, 8 \rangle$	$\langle -90, 6 \rangle$
$f_1 [\text{Hz}]$	$55.43^{+1.37\%}$	$54.99^{+0.57\%}$	$54.98^{+0.55\%}$
mass [kg]	$0.4591^{-12.5\%}$	$0.4591^{-12.5\%}$	$0.4591^{-12.5\%}$

Table 1 presents the results of the multi-objective optimization for the unconstrained problem. As the structural theory is varied, the optimal lamination angles are shown. In addition, the implementation of VAT composites allows the use of a symmetrical 7-layer laminate, resulting in a mass reduction of 12.5% while maintaining approximately the same fundamental frequency as the reference model.

Table 2. Optimal design results for the constrained problem ( $\kappa_{lim} = 3.28 \text{ m}^{-1}$ )

	ESL – TE 1	ESL – TE 3	LW – LD2
$\langle T_0, T_1 \rangle^1 [^\circ]$	$\langle -86, -31 \rangle$	$\langle -85, -31 \rangle$	$\langle -85, -30 \rangle$
$\langle T_0, T_1 \rangle^2 [^\circ]$	$\langle 79, 26 \rangle$	$\langle 72, 22 \rangle$	$\langle 76, 25 \rangle$
$\langle T_0, T_1 \rangle^3 [^\circ]$	$\langle -60, -12 \rangle$	$\langle -61, -13 \rangle$	$\langle -61, -13 \rangle$
$\langle T_0, T_1 \rangle^4 [^\circ]$	$\langle 58, 10 \rangle$	$\langle 70, 20 \rangle$	$\langle 62, 15 \rangle$
$f_1 [\text{Hz}]$	$52.42^{-4.12\%}$	$52.06^{-4.79\%}$	$52.01^{-4.87\%}$
mass [kg]	$0.4591^{-12.5\%}$	$0.4591^{-12.5\%}$	$0.4591^{-12.5\%}$

As described in Section 3, Table 2 displays the optimal results for the constrained problem for both ESL and LW models. Similar to the previous case, a 12.5% reduction in mass is observed.

However, due to the significant decrease in the design domain resulting from the limitation of the maximum bending radius of the AFP machine, the natural frequency is reduced by slightly more than 4% with respect to the reference.

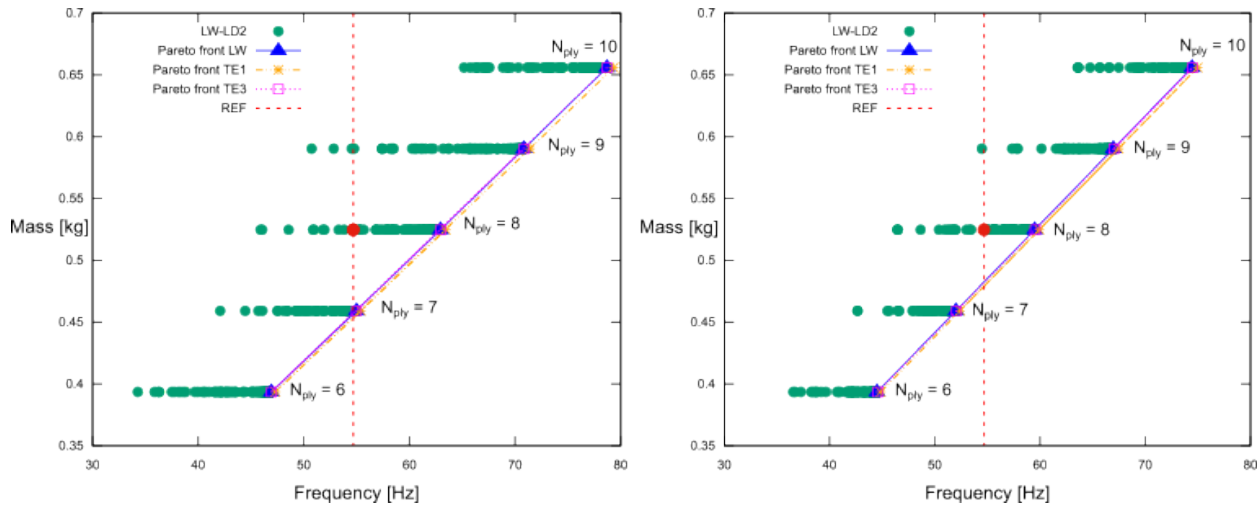


Figure 1. Pareto fronts for the unconstrained case (on the left) and for the constrained case (on the right)

Figure 1 displays the Pareto fronts for the unconstrained and constrained problem as the structural theory changes. It should be noted that the mixed-integer optimization strategy produces discontinuous response surfaces, allowing each layer to be optimized independently. In the unconstrained case, achieving the same optimum frequency as the reference utilizing a layer less is possible. However, in the constrained case, this is not possible. Nevertheless, it is noted that it is feasible to obtain much higher frequencies, but with the same mass as the reference

### Conclusions

This work presented a mixed-integer optimization framework for the least-weight design of VSCs, taking into account the design space restriction resulting from the AFP manufacturing process. As demonstrated in [3], the structural theory exhibits a weak dependence on the optimal lamination angles for each layer. Moreover, layer-wise optimization provides discontinuous response surfaces, enabling the implementation of high-fidelity models that offer significant advantages over alternative optimization approaches.

### References

- [1] Groh, R.M., Weaver, P.: Mass optimisation of variable angle tow, variable thickness panels with static failure and buckling constraints. In: 56thAIAA/ ASCE/AHS/ASC Structures, Structural Dynamics, and Materials Conference (2015). <https://doi.org/10.2514/6.2015-0452>
- [2] Catapano, A., Montemurro, M., Balcou, J. – A., Panettieri, E.: Rapid prototyping of variable angle-tow composites. *Aerotecnica Missili e Spazio* 98(4), 257-271 (2019). <https://doi.org/10.1007/s42496-019-00019-0>
- [3] Racionero Sánchez-Majano, A., Pagani, A.: Buckling and fundamental frequency optimization of tow-steered composites using layerwise structural models. *AIAA Journal* 61(9), 4149–4163 (2023). <https://doi.org/10.2514/1.j062976>
- [4] Pagani, A., Racionero Sánchez-Majano, A., Zamani, D., Petrolo, M., Carrera, E.: Fundamental frequency layer-wise optimization of tow-steered composites considering gaps and overlaps. *Aerotecnica Missili e Spazio* (2024). (Under review)

- [5] Fayazbakhsh, K., Nik, M. A., Pasini, D., Lessard, L.: Defect layer method to capture effect of gaps and overlaps in variable stiffness laminates made by automated fiber placement. *Composite Structure* 97 (2013), 245-251. <https://doi.org/10.1016/j.compstruct.2012.10.031>
- [6] Carrera, E., Cinefra, M., Petrolo, M., Zappino, E.: *Finite Element Analysis of Structures through Unified Formulation*. Wiley & Sons, Hoboken, New Jersey. 2014.
- [7] Gürdal, Z., Tatting, B.F., Wu, C.K.: Variable stiffness composite panels: Effects of stiffness variation on the in-plane and buckling response. *Composites Part A: Applied Science and Manufacturing* 39(5), 911–922 (2008). <https://doi.org/10.1016/j.compositesa.2007.11.015>
- [8] Carvalho, J., Sohouli, A., Suleman, A.: Fundamental Frequency Optimization of Variable Angle Tow Laminates with Embedded Gap Defects. *Journal of Composites Science* 6, 64 (2022). <https://doi.org/10.3390/jcs6020064>